Supplementary Information

Genome-wide Single-cell-level Screen for Protein Abundance and Localization Changes in Response to DNA damage in *S. cerevisiae*

Aprotim Mazumder[1,2,5], Laia Quiros Pesudo[1,2], Siobhan McRee[1,2], Mark Bathe[1,2,5], Leona D. Samson[1,2,3,4,*]

[1]Department of Biological Engineering, [2]Center for Environmental Health Sciences, [3]Department of Biology, [4]The David H. Koch Institute for Integrative Cancer Research, [5]Laboratory for Computational Biology and Biophysics, Massachusetts Institute of Technology, Cambridge, MA 02139, USA

[*]To whom correspondence should be addressed: lsamson@mit.edu

Rationale for developing an optimized fixation method.

In the past two decades the use of green fluorescent protein (GFP) technology has revolutionized biology (1,2). A prime strength of this approach is the ability to visualize dynamic processes in live cells with proteins of interest genetically tagged with GFP. While the application of GFP technology is usually limited to studies of candidate proteins of interest, the ready availability of libraries of GFP clones in many systems has brought GFP technology into the realm of wider screens involving many genes. For example a budding yeast (*Saccharomyces cerevisiae*) library has been developed in which nearly 70% of the yeast proteome is tagged with a GFP label at the C-terminal (3). A key advantage of this system is that the proteins are expressed to endogenous levels and hence are not subject to artifacts due to over-expression. This library has been used for both studying protein localization using microscopy (3) and levels using flow cytometry (4), demonstrating the possibility for large-scale screens. Traditionally fixed mammalian cells have been used to study the effects of drug perturbations on cells using imaging-based High Content Screening (HCS). Fixation is essential for investigating specific time-points across a large number of clones. Additionally fixation also allows the simultaneous immunofluorescent staining of different cellular compartments, and imaging in media with lesser background fluorescence than the growth media required by live cells. However, a major caveat of fixation while working with GFP is that most fixation techniques generally attenuate GFP signals. GFP fluorescence has been shown to be resistant to fixation by alcohol or aldehydes to a certain extent (5,6). Some studies have indicated that alcohol-based fixations are more detrimental to GFP signals (7,8), and also additionally membrane permeabilization in alcohol-based fixation can cause the release of soluble pools unbound GFP-tagged proteins (5,9). Thus aldehyde-based fixation methods may be preferable for best-preserving GFP signals. For relatively highly expressed proteins subcellular localization can still be discerned despite the attenuation of the signal, but an understanding of the nature of the signal loss across the expression range is necessary for comparing even the relative levels of tagged proteins. This becomes a particular concern when proteins are expressed at very low levels close to cellular autofluorescence, as is true for expression from most endogenous promoters. When investigating individual proteins of interest, in addition to looking at GFP signals directly in fixed cells, some studies choose to perform an immunofluorescence-based detection of the GFP (5,6), but this becomes unviable in large-scale screen. Moreover the low numerical aperture (NA) air objectives usually used in HCS, are less efficient in detecting weak

signals than high magnification, high NA objectives that could be used in confocal microscopy of individual candidate proteins .

For these reasons it is essential to choose a fixation process which causes the minimal possible loss of GFP signal. As a part of the larger screen for cellular response in yeast to MMS, we compared two aldehyde-based fixation methods that have been previously described in the literature specifically for use in yeast strains expressing GFP-tagged fusion proteins. We compared these with both flow cytometry and imaging-based detection of protein levels.

Cell fixation protocols. Fixation protocol 1 (Fix 1) (adapted from a previous study (6)): 100 μl of the culture was treated with an equal volume of freshly made aqueous solution containing 250 mM potassium phosphate, 2 mM magnesium chloride, 4% formaldehyde (FA), and 0.5% glutaraldehyde. Cells were then centrifuged at 1500 g and resuspended in phosphate buffered saline (PBS). This protocol was used to look at Golgi structure in yeast cells. These authors used GFP fluorescence directly and also used an anti-GFP antibody to augment signals, when performing immunofluorescence with another antibody. Such an approach would be both time and resource intensive in a high throughput study, and it was desirable that GFP fluorescence can be used directly. Attenuated GFP signals can be perhaps used for specifying localization of a high-expressed protein, but determining levels would be problematic. Moreover most of the strains in the yeast GFP library were expressed to low levels being driven by endogenous promoters. Hence signal loss would be even more of a concern.

Fixation protocol 2 (Fix 2) (adapted from a previous study (10)): Cells were suspended in 100 μl 4% paraformaldehyde (PFA), 3.4% Sucrose in PBS and allowed to stand for 30 minutes. Cells were then washed once in potassium phosphate buffer with 1.2 M sorbitol and resuspended in PBS. This protocol was adapted from a study in yeast looking at microtubule binding at kinetochores. A key difference in this fixation procedure was that paraformaldehyde was used as a fixative, and unlike standard formaldehyde solutions this does not contain methanol, which attenuates fluorescence signals, and can cause cytosolic proteins to escape from the cell by compromising plasma membrane integrity (5). Moreover it does not employ glutaraldehyde as a fixative, which was known to raise cellular autoflorescence levels by slow build-up of its own fluorescence (11). This was the method of choice followed for fixing the cells in the screen for reasons explained in Supplementary Figures 3 - 5 below.

Detailed Protocol for Processing Plates for High Content Imaging

Supplies:

1. 2.0ml Deep Well Square Plate (Axygen, cat # 22-491)
2. 'Breathable' sealing films or tops (Genesee)
3. 96 Well Optical Bottom Black Plates (Nunc, cat # 265301)
4. Black sealing tape for Optical plates (Cole-Parmer, cat # 600187)
5. 96 Well flat bottom plates (Costar, cat # 3585)
6. 96 Well round bottom plates (Costar, cat # 3367)
7. ConA-Alexa647 (Invitrogen, cat # C21421)
8. Concanavalin A for plates (Sigma, cat # C7275)
9. MMS (methyl methanesulfonate) (Sigma, cat # 129925-25G)
10. SC - His medium (MP biomedicals, cat # 4410-222)
11. SC medium (MP biomedicals, cat # 4400-022)

The media formulations were the same as previously described(4). We processed 12 plates per three days, equivalent to 2 plates from the GFP library (3 replicates of control and MMS-treated samples for each treatment). The protocol is divided into 2 days. On the first day, the samples were treated or not, fixed, and kept at 4 ˚C wrapped in aluminum foil. On the second day the cells were stained with DAPI and ConA-Alexa647 in preparation for imaging on the Cellomics system.

1. Three days before the experiment, 2 plates were pinned in 200µl SD-His with the pin tool and incubated for 3 days at 30 ˚C (without shaking).
   Each plate included controls strains in fixed positions. The WT strain served as an autofluorescence control. Hug1-GFP was chosen as it was maximally induced in an earlier study(12). Rnr4-GFP serves both as a control for both level and localization changes.
2. In the evening, 30,000 cells were inoculated in 600 µl SD+AA (SD medium supplemented with the amino acids His, Leu, Ura, Met) in 2ml Deep-well plates by Pre-diluting the 3 day culture (20ul in 180ul) and subsequently adding 3ul in 600ul. The WT strain was always grown in SD+AA.
3. Cells were grown overnight (15h, approx. 7 doubling times) at 30˚C with shaking. Deep-well plates were covered with 'Breathable' Sealing Films.

4. Next morning, the culture is expected to be in early log phase with an OD 600 between 0.4 and 0.8 ($8X10^6$/ml and $1.6X10^7$cells/ml). For the treated plates, 500ul of the overnight culture was taken and 100ul of 0.12% MMS diluted in SD+AA was added to obtain a final concentration of 0.02% MMS. For the untreated control plates, 100ul SD+AA was added. Plates were incubated at 30˚C with shaking for 3 hrs.
5. After 3 hrs, 300ul of culture was from each plate and centrifuged for 5 min at 2500 rpm.
6. 150 μl of the supernatant was discarded and 150ul of 2X fixative was added, mixed and incubated for 30 min at room temperature.
7. After incubation, cell were centrifuged for 5 min at 2500 rpm and the supernatant removed. Samples were washed twice with KPO_4 / Sorbitol, and resuspended in 200ul KPO_4 / Sorbitol. At this point, the sample might be stored at 4 ˚C wrapped in aluminum foil.
8. Samples were centrifuged and the supernatant removed. 200ul of staining mixture (1 ug/ml DAPI and 200 ug/ml ConcanavalinA-Alexa647 in PBS) was added and staining was carried out for 30 min at room temperature covered with aluminum foil. Samples were then centrifuged and washed twice in PBS.
9. 100ul PBS was added and the cells transferred to NUNC optical bottom plates treated with strength 100 μg/ml Concanavalin A. It is best to let the cells sit for at least 5 min, and no longer than 20 min.
10. The culture was shaken off and 100ul PBS was added to each of the wells to wash away the unstuck, free-floating cells. Cells were washed gently (manually), and PBS was added along the walls of the wells without touching the bottom of the well with the tip. This step can be repeated if the bottom looks dense.
11. Finally 100ul PBS/30% glycerol was added and plates sealed with black sealing tape.

Solutions:

1M KH_2PO_4

68g in 500mL of warm water

1M K_2HPO_4

87g in 500mL of water

2M Sorbitol

182g in 500mL of warm water

1M Potassium Phosphate KPO_4

83.4mL 1M K_2HPO_4

16.6mL 1M KH_2PO_4

KPO_4/Sorbitol

60mL 2M Sorbitol

10mL 1M Potassium phosphate

30mL water

2X Fixative: 4% Paraformaldehyde 3.4% Sucrose in PBS

100 ml: 8g PFA powder

6.8g Sucrose

10 ml 10X PBS

Make the volume to 100 ml with MQ water

Perform stirring and heating in a fume hood (the vapors are noxious)

Cell Staining Mixture in 1X PBS

1-2 microgram/ml DAPI

5 microgram/ml Concanavalin A -Alexa 647

Additional note on Statistical Analyses.

The use of Kolmogorov-Smirnov (KS) statistics. KS statistics is widely used in High Content Screening and a value of >0.2 may represent significant differences (13-19). The one sample KS test is used to compare a sample measurement on a population to an expected distribution. However, the two sample KS test compares two distributions without any assumption of their form (20). Without a correction, the p-value obtained from KS tests (or any statistical test for that matter) tends to be artificially small given the large number of samples obtained in a screen, leading to spurious false positives, whereas the distance between the normalized cumulative distribution functions is a more robust measure of meaningful differences. Cell numbers vary from sample to sample, and this must be accounted for by attributing greater weight to samples with larger numbers of cells using the critical value c(α) (20,21). For example, if the number of cells in a control sample is m and in a drug-treated sample is n, the null hypothesis that the two distributions are drawn from the same underlying distribution is rejected at a level α if the KS statistic $D_{m,n}$ is such that,

$$D_{m,n} > c(\alpha)\sqrt{\frac{m+n}{mn}}$$

i.e.

$$c(\alpha) < C_{m,n}, where\ C_{m,n} = D_{m,n}\sqrt{\frac{mn}{m+n}}$$

The value of c(α) is given in the table below for each level of α

α	0.10	0.05	0.025	0.01	0.005	0.001
c(α)	1.22	1.36	1.48	1.63	1.73	1.95

In the present study we calculated not only the KS statistic $D_{m,n}$, but also the factor $C_{m,n.}$ Because using only the condition $C_{m,n}$ >1.95 results in an inordinately high number of hits, we instead used the KS statistic cut-off of 0.3. While this is more stringent than at cut-off of 0.2, it is

still arbitrary; but importantly, every strain that passed this criterion also passed the less stringent criterion $C_{m,n}$ >1.95. The $C_{m,n}$ for all the responder strains are specified in Supplementary Table 1.

The use of t tests and other statistical tests. Three means of the control samples for a strain were compared to three means of the corresponding MMS-treated samples with a Student's t-test. The null hypothesis was that the means are not different. For small sample sizes in fact the t test is widely regarded as the appropriate test with Bonferroni or Benjamini-Hochberg corrections made for large sample sizes. A seminal work suggests that in case of multiple comparisons, corrections not be performed and the fact be stated (22). For the Gene Ontology where large numbers of genes are compared to determine relative enrichment of processes, a recommended Benjamini-Hochberg correction of the p-values is performed. The enrichment was relative to the whole proteome both for the GO analysis and also for the calculation of 'normalized occurrence' for each TF.

Supplementary Figures and Figure Legends

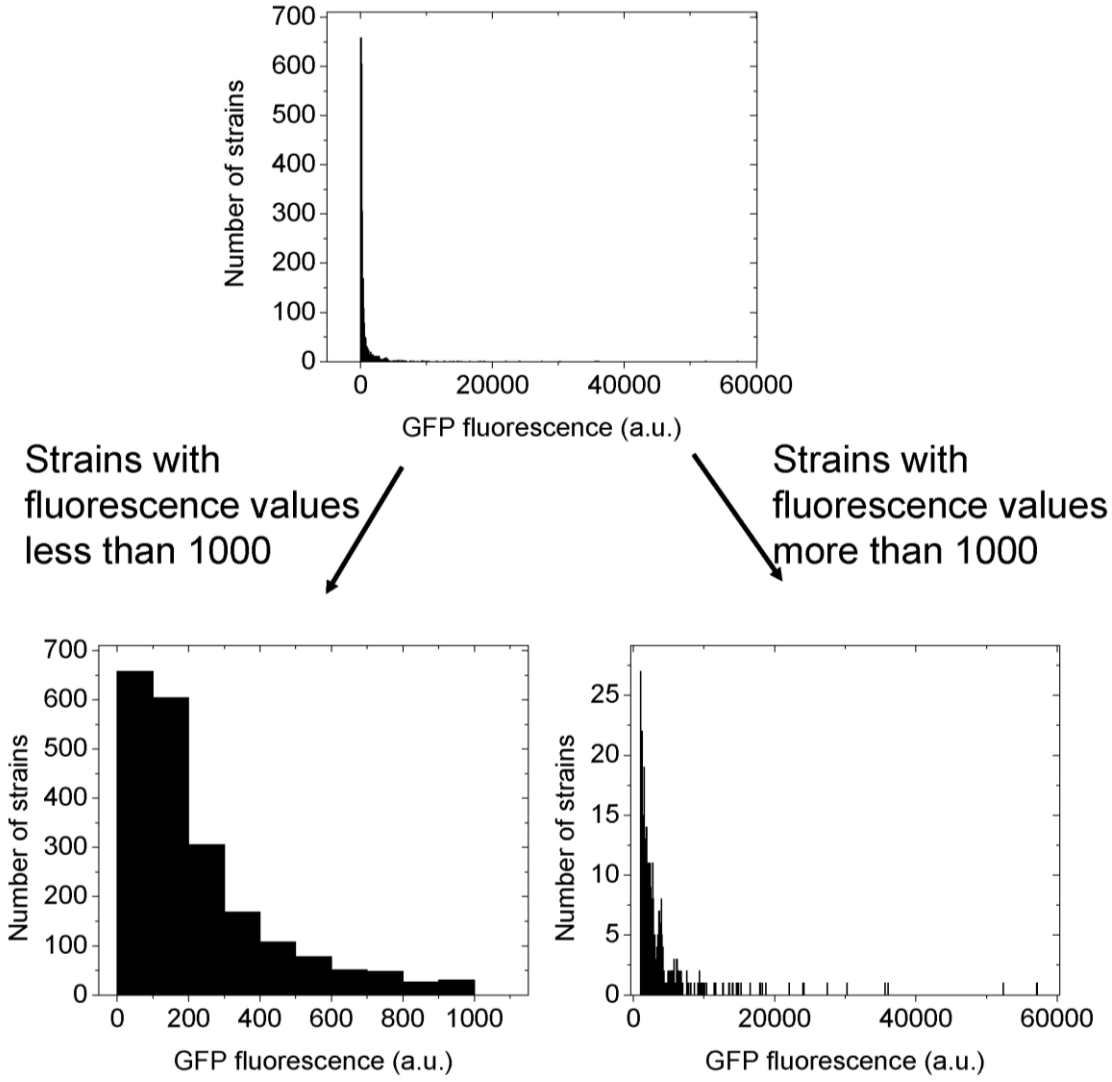

Supplementary Figure 1. Expression range of proteins in GFP library. In the study by Newman et al, characterizing protein levels in the yeast GFP library, the fluorescence from 2450 strains out of 4159 could be reliably measured in SD-His medium. While the measured fluorescence values after autofluorescence correction ranged from 48 to ~57000 (in arbitrary units (a.u.)), only ~15% of the 2450 strains (372/2450) had values above 1000. The histograms above are plotted using data from the work by Newman et al (4). The histogram on top shows the average GFP fluorescence for different stains for all of the 2450 strains measured. Because

there are relatively fewer strains with high GFP-expression, this histogram is divided into two parts shown in the bottom. For direct comparison the bin-size is maintained constant at 100 for all three histograms.

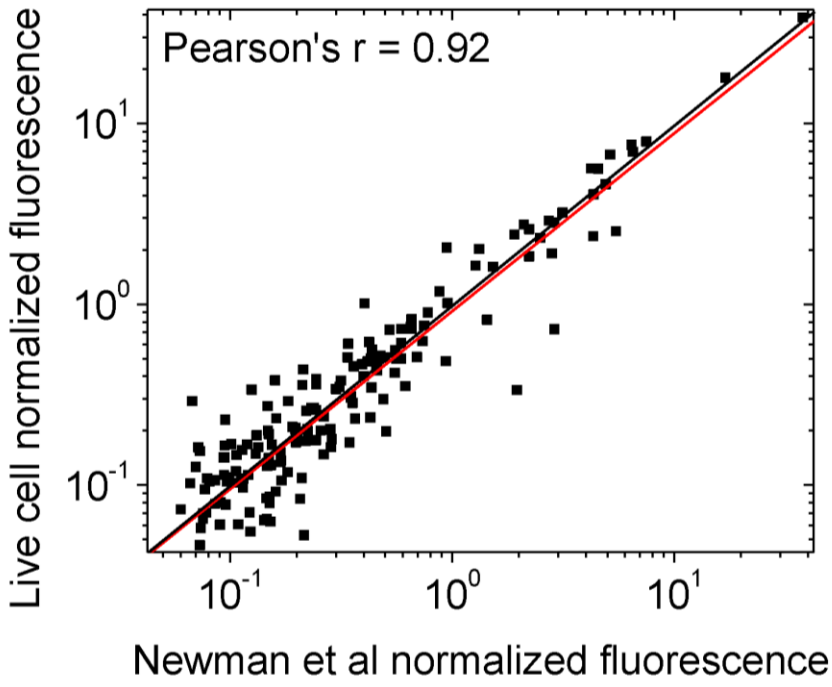

Supplementary Figure 2. Comparison of live cell fluorescence from flow cytometry with Newman et al. Comparison of live cell median fluorescence values with those reported by Newman et al (4) for the same strains grown in SD-His medium using flow cytometry. The black line is the 1:1 line, while the red line shows the linear fit. Values for any one method are normalized by the mean fluorescence of all the strains compared to allow for direct comparison of relative fluorescence levels. Of the 204 strains used, values for 181 could be found in the experiments of Newman et al. This shows that under the culture conditions used by us the fusion GFP expression is as expected.

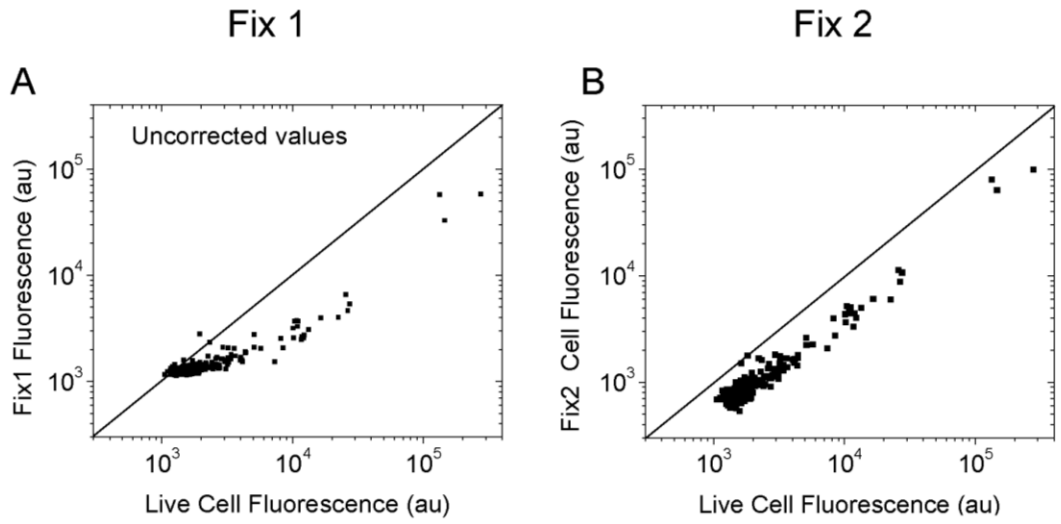

Supplementary Figure 3. Comparison of live and fixed cell fluorescence by flow cytometry shows the attenuation of GFP fluorescence signal upon fixation for the two protocols investigated. Raw uncorrected fluorescence values are plotted for (A) Fix 1 and (B) Fix 2. Each data point represents the median fluorescence for a strain from the library. 204 strains are compared. Note the non-linear nature of the scatter of the points for Fix 1. The cause for this is further explored in Supplementary Figure 4, 5. The black line is the 1:1 line. Both fixation methods show loss of fluorescence (the scatter is below the 1:1 line), but the loss is linear only for Fix 2.

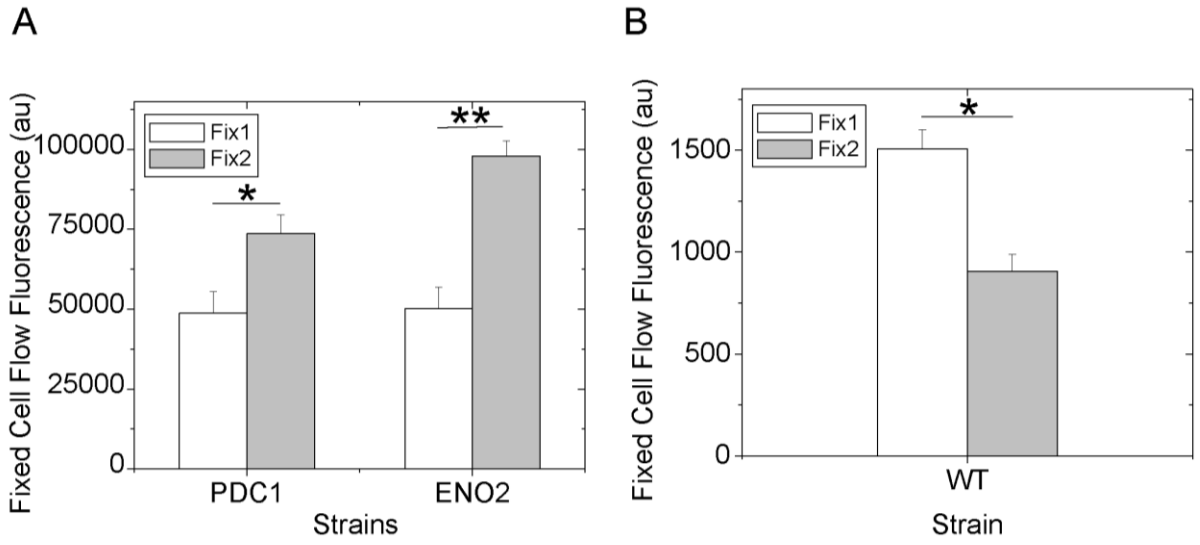

Supplementary Figure 4. Effects of the fixatives on specific strains at different expression levels. Greater loss of GFP fluorescence and elevation of cellular autofluorescence (AF) for Fix 1 differentially affects the two ends of the range of protein expression, as evaluated

by flow cytometry on fixed samples. Raw fluorescence values are plotted. (A) For higher expressed proteins the GFP signal loss is greater for Fix 1 than for Fix 2. PDC1 and ENO2 are two most highly expressed proteins in the GFP library (4). (B) The basal AF levels are also elevated for Fix 1, as seen here for the parental wildtype (WT) strain. These two effects in (A) and (B) affect the two ends of expression differently - GFP signal loss dominates at high expression levels for Fix 1, but this masked by elevated AF levels as expression levels approach WT AF. This also causes the non-linear nature of the scatter in Supplementary Figure 3A, as more low-expressing strains become comparable to the higher basal AF. This also causes fewer strains to be reliably measured after AF correction. Such a non-linear compression of the range of expression (fluorescence loss at the high-end, and more strains becoming comparable to the WT at the low-end) makes reliable discrimination of true GFP fluorescence levels more difficult for Fix 1. Means and standard deviations over triplicate experiments are plotted. * indicates $p<0.01$ and ** indicates $p<0.001$ in a Student's t-test.

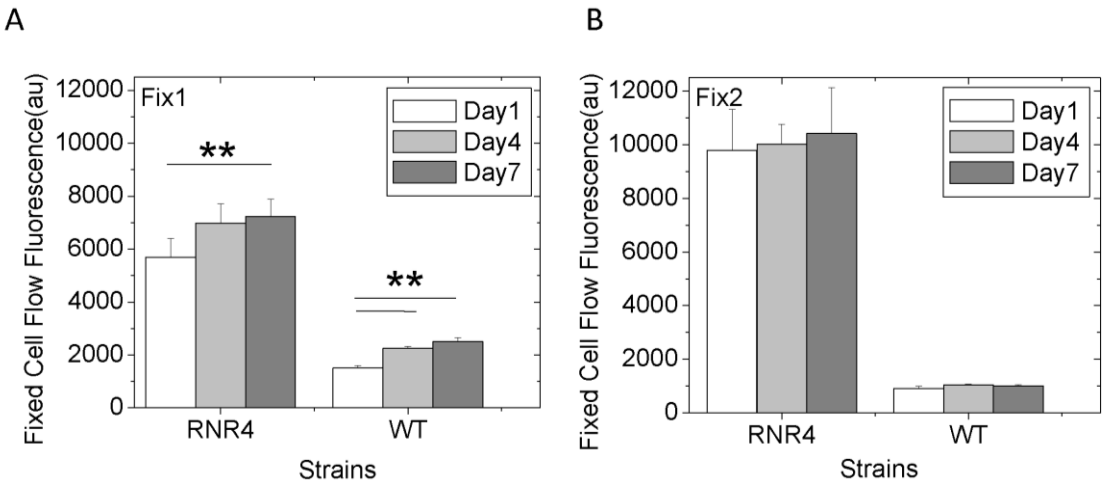

Supplementary Figure 5. Changes in fluorescence of fixed samples with time also indicate Fix 2 to be more desirable. (A) Strains including WT cells show gradual rise in fluorescence with time. This is attributed to previously reported development of fluorescence in glutaraldehyde-fixed samples (11). Trends are shown for a medium expression level protein (Rnr4) and the WT strain. (B) Samples fixed by Fix 2 are relatively more constant in fluorescence levels in the same time-course. Loss of fluorescence due to sample degradation is also not apparent. Values shown are means of the three flow-cytometry experiments, and error-bars denote standard deviations. ** indicates $p<0.001$ in a Student's t-test.

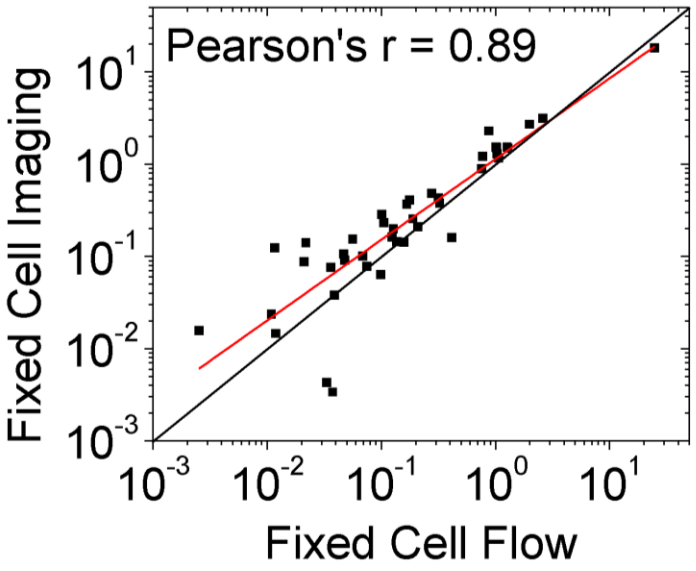

Supplementary Figure 6. Comparison of Fixed Cell Flow and Fixed Cell Imaging for Fix 2. GFP fusion protein fluorescence from 42 strains are compared by fixed cell flow cytometry and fixed cell imaging. The fixation method of choice (Fix 2) is used. The black line is the 1:1 line, while the red line shows the linear fit. AF-corrected values are used. Values for any one method are normalized by the mean fluorescence of all the strains compared to allow for direct comparison of relative fluorescence levels.

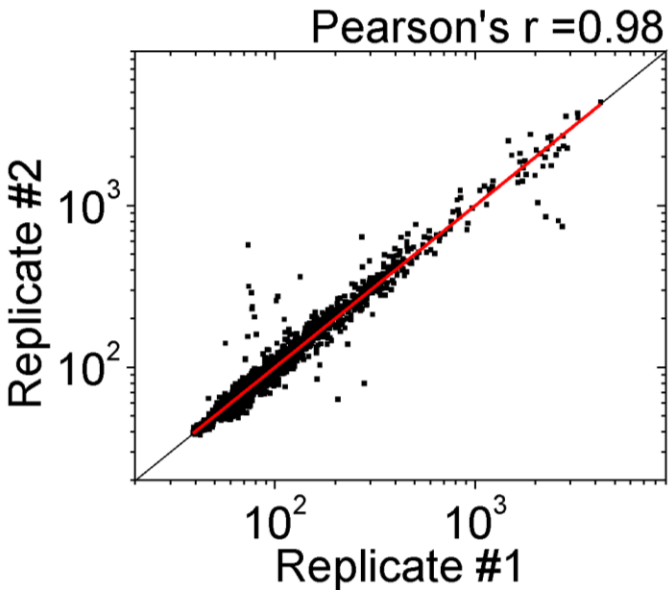

Supplementary Figure 7. Comparison of replicates in the present study. Raw fluorescence measurements for every measured strain in the present study are plotted against each other for two untreated replicates. The red line is a linear fit, while the black line is a 1:1 line.

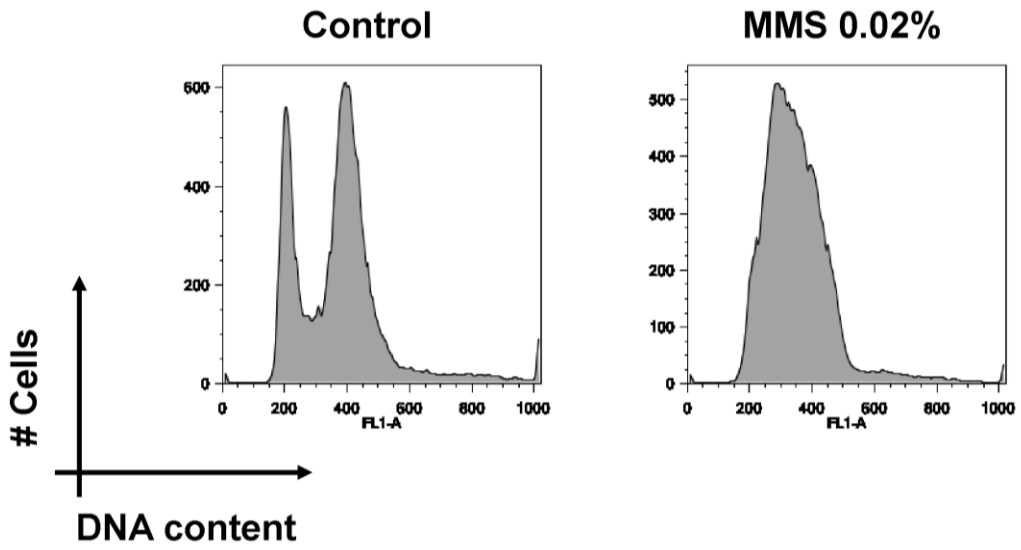

Supplementary Figure 8. Cell-cycle profiles of BY4741 cells with and without treatment with 0.02% MMS for 3 hours. Cells pause in the S-phase to repair the damage caused by MMS. Exponentially growing cultures were stained with Sytox green following previously described protocols (23). 30,000 cells were counted for each profile. These experiments were performed on a FACSCalibur flow cytometer.

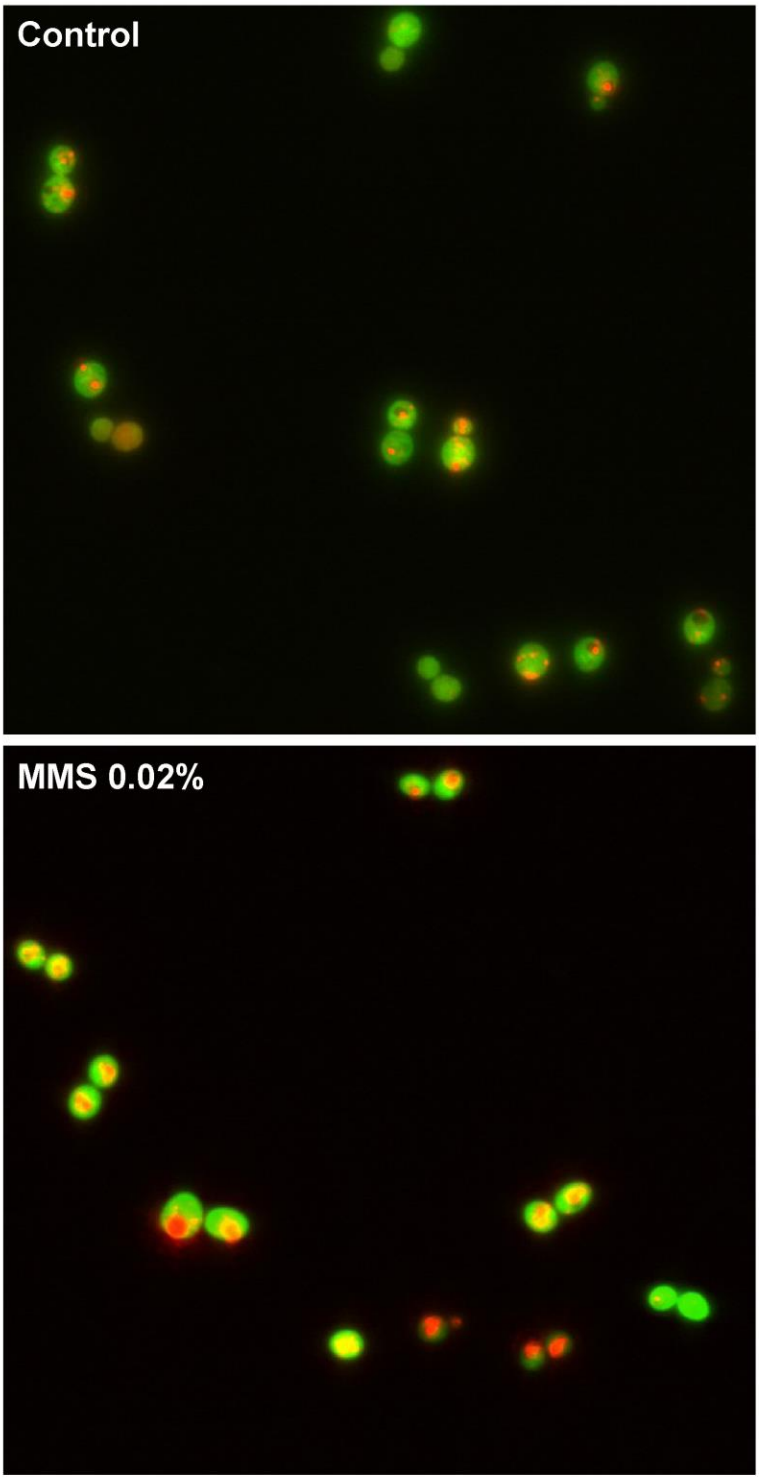

Supplementary Figure 9. Vitality stains of BY4741 cells with and without treatment with 0.02% MMS for 3 hours. FUN1 staining was performed following the manufacturer's protocol. All cells (dead and alive) are stained green by the stain, but only alive cells can process the dye

to generate red internal structures. No excessive cell death was observed at the 3 hour time point for the MMS-treated sample.

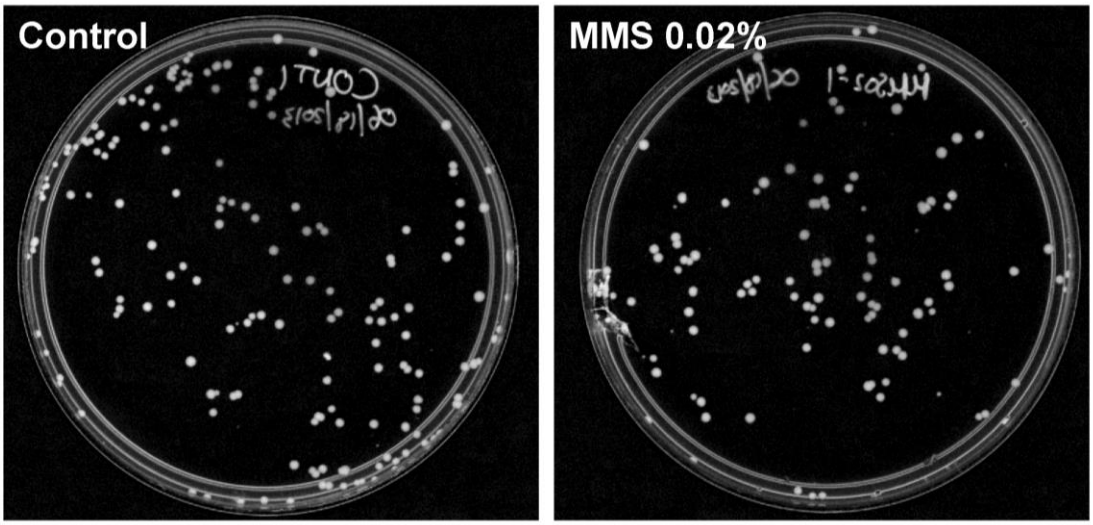

Supplementary Figure 10. Colony forming ability of cells with and without treatment with 0.02% MMS for 3 hours. Following MMS-treatment, cells were washed and equal numbers plated of YPD-agar plates in triplicate. A typical example is shown above. Overall the MMS plates showed 60% the number of colonies compared to untreated samples.

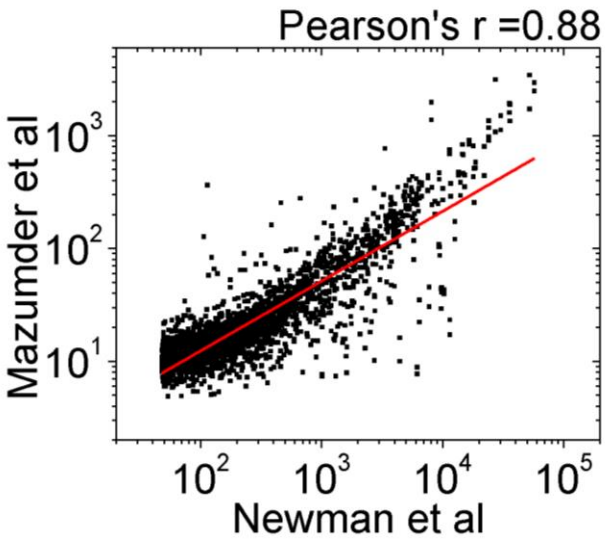

Supplementary Figure 11. Comparison of protein abundance measurements in our study with that by Newman et al. Newman et al (4) reported the measurement on a subset of GFP-tagged strains by live cell flow cytometry. Reported values for strains are plotted against each other for that study and the present one without any manipulation. The units are different on the two axes given that different assays are used. Both are measurements of fluorescence in arbitrary units. Given that our study is performed in fixed cells and by imaging, the correlation is surprisingly good. The Pearson's r value of 0.88 is comparable (0.89) to that reported by Tkach et al (24) who used live cells for imaging. The red line shows a linear fit.

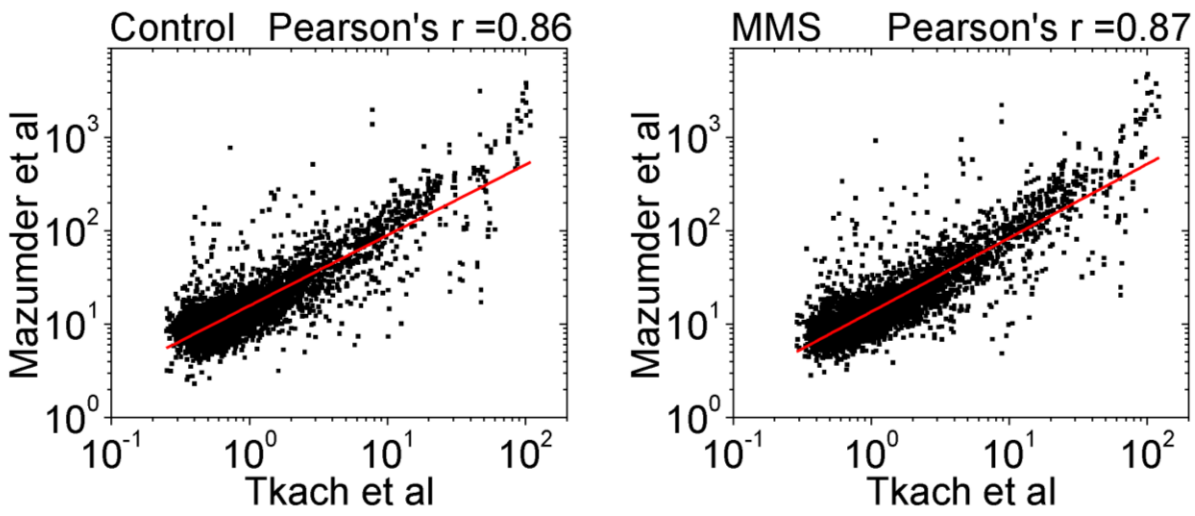

Supplementary Figure 12. Comparison of protein abundance measurements in our study with that by Tkach et al. Tkach et al (24) reported the measurement on all GFP-tagged strains by live cell imaging. Reported values for strains are plotted against each other for that study and the present one without any manipulation. The units are different on the two axes because different assays are used. Both are measurements of fluorescence in arbitrary units. For both Control and MMS treated samples a good-correlation is seen. Bear in mind the study by Tkach et al used 0.03% MMS for 2 hours, while we used 0.02% MMS for 2 hours. Despite this the general correlation holds. The red lines show linear fits.

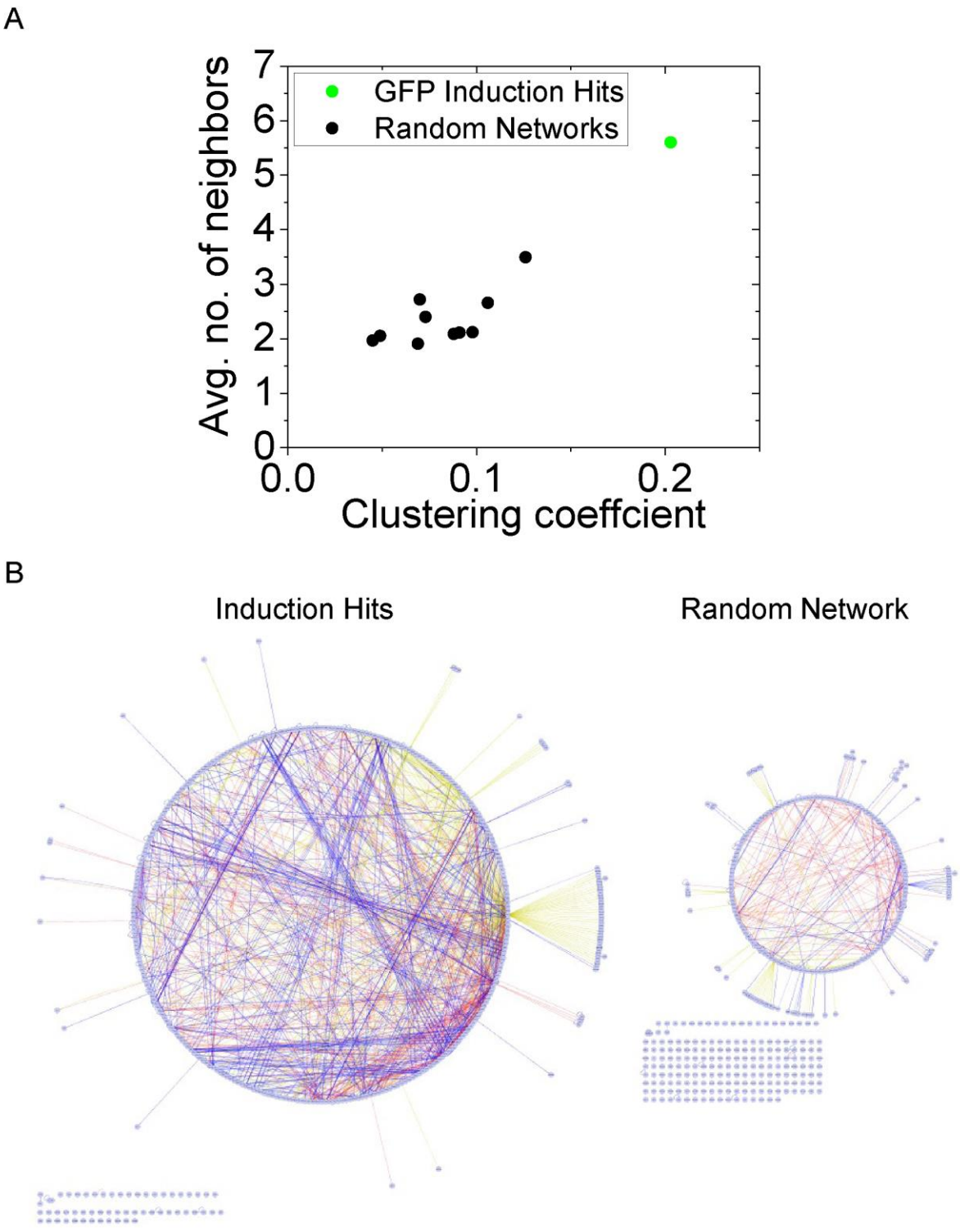

Supplementary Figure 13. Comparison of the network of induced proteins to random networks of the same size. (A) The average number of neighbors and is plotted against the clustering coefficient for the total network of induced proteins (green circle) and ten random

networks of the same size (black circles). Induced proteins show higher average number of neighbors ($p=1.4X10^{-4}$) and clustering coefficient ($p=1.3X10^{-3}$) than the random networks. (B) The network of induced proteins and a typical random network are laid out in a circular layout in Cytoscape. Blue, red and yellow edges represent physical, genetic and TF interactions respectively. The same number of nodes are present in the networks; note the much bigger large connected component (LCC; 354/410 nodes) and fewer isolated nodes for the induced versus random proteins.

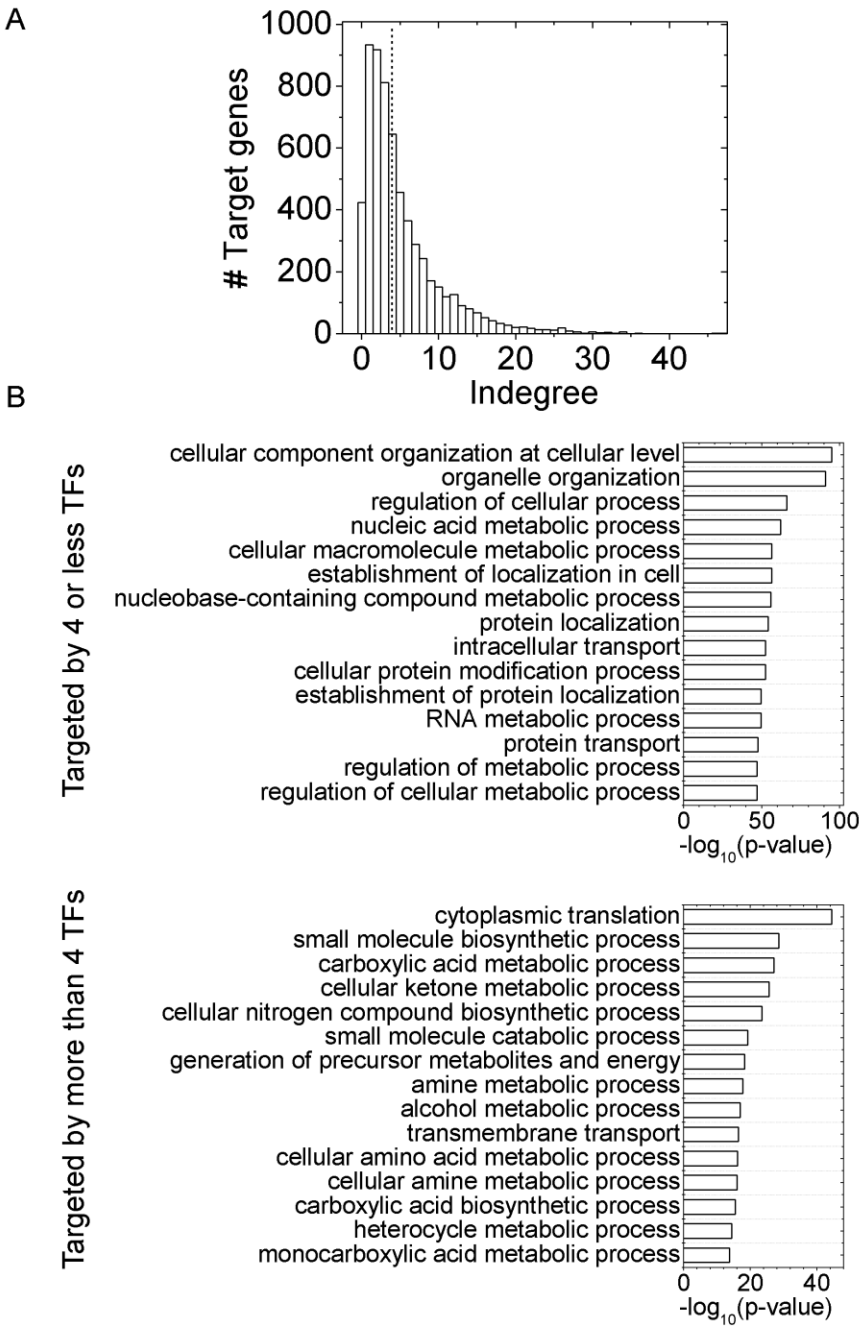

Supplementary Figure 14. Function according to indegree in the full yeast transcriptional network. (A) Even in the full yeast transcriptional network the median value of indegree is 4 (see Figure 3B for the indegree distribution for the induced proteins). (B) When partitioned according to indegree (i.e. the number of TFs targeting the expression of a protein), metabolic processes continue to dominate the nodes with higher indegree.

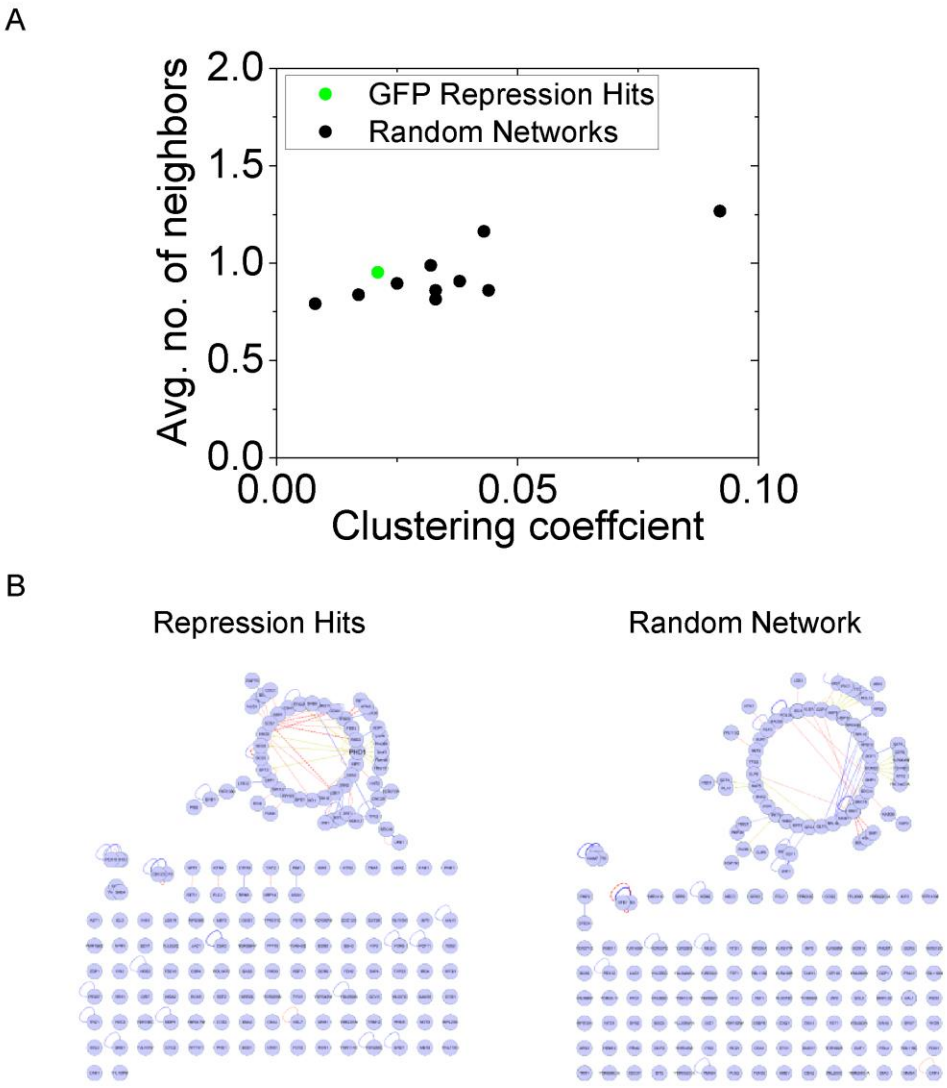

Supplementary Figure 15. Comparison of the network of repressed proteins to random networks of the same size. (A) The network of repressed proteins shows similar average number of neighbors and clustering coefficients when compared to ten random networks of the same size. (B) The network of repressed proteins and a typical random network are presented in a circular layout in Cytoscape. The same number of nodes is present in both networks; there is no striking visual difference between the two networks. All representations are similar to Supplementary Figure 6.

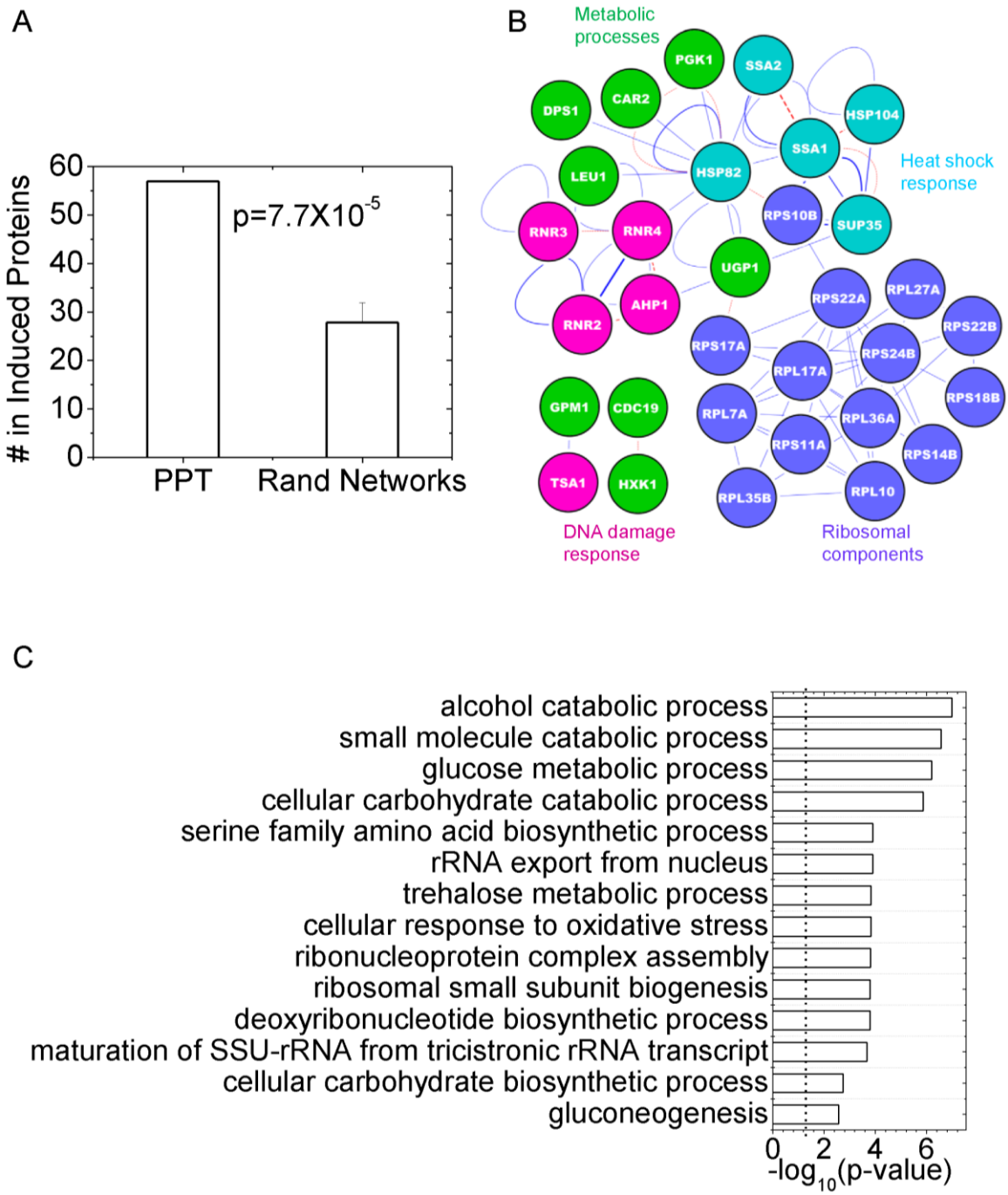

Supplementary Figure 16. Signatures of translational regulation of the induced proteins. (A) 57 proteins of the PPT group (called Group 1 in (25)) are induced, twice what is expected by random chance. The error bar is standard deviation for 10 Random networks of the same size, the mean of which is like what is theoretically expected. (B) The 57 common proteins form a large connected group (isolated nodes not shown). (C) GO analysis of the 57 genes – note processes related to carbohydrate, trehalose metabolism, ribosomes, oxidative stress and dNTP production.

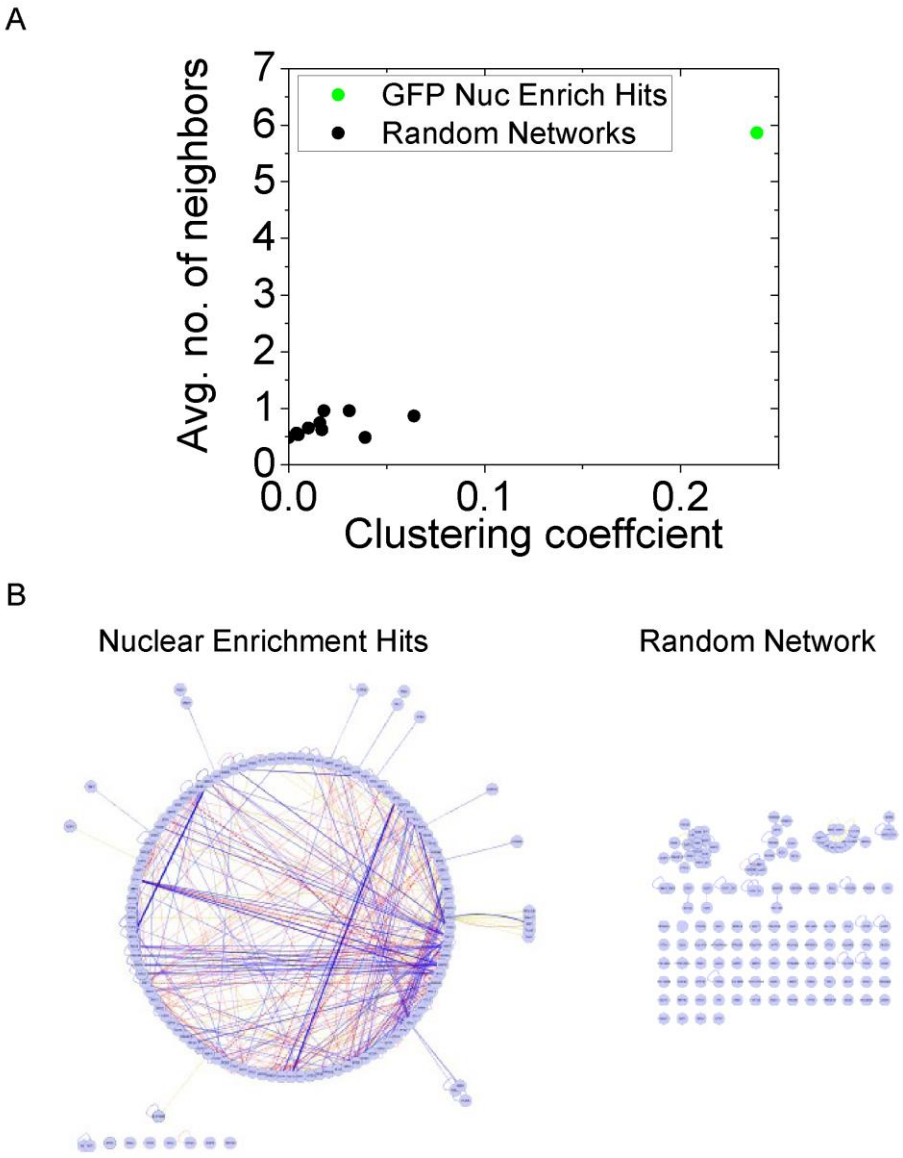

Supplementary Figure 17. Comparison of the network of nucleus-enriched proteins to random networks of the same size. (A) The network of nucleus-enriched proteins show much higher average number of neighbors ($p=6.8X10^{-10}$) and clustering coefficient ($p=2.1X10^{-6}$), than ten random networks of the same size. (B) The network of nucleus-enriched proteins and a typical random network are presented in a circular layout in Cytoscape. The same number of nodes are present in the networks; note the much bigger large connected component (LCC; 123/132 nodes) and fewer isolated nodes for the nuclear-enriched versus random proteins. All representations are similar to Supplementary Figure 6.

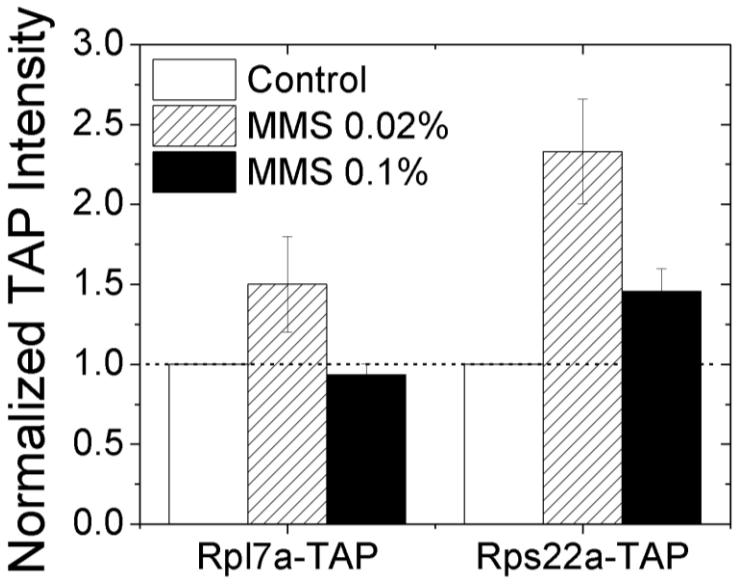

Supplementary Figure 18. Strains expressing TAP-tagged Rpl7a and Rps22a also evidence an induction of the tagged proteins when treated for two hours with 0.02% MMS. Rpl7a and Rps22a strains from the TAP-tagged library were used to confirm the induction response at 0.02% MMS. The TAP-tag was detected with a Rabbit Anti-GFP-Alexa647 antibody and levels quantified by flow cytometry. The protein A portion of the TAP tag has a great affinity for the Rabbit IgG, no matter what the antibody is raised against. This has been previously exploited for the detection of TAP tags (26,27). Independent experiments showed that the TAP-tagged strains showed much higher staining intensity with this antibody than parental WT strains – clearly indicating this is a specific recognition. The subtle repression of protein levels at 0.1% MMS was not apparent possibly due to variations in staining conditions or longer protein half-lives, but the induction at 0.02% was clear. The mean and standard deviations from two independent experiments performed on different days are shown. For each experiment the intensity of the control samples are normalized to 1.

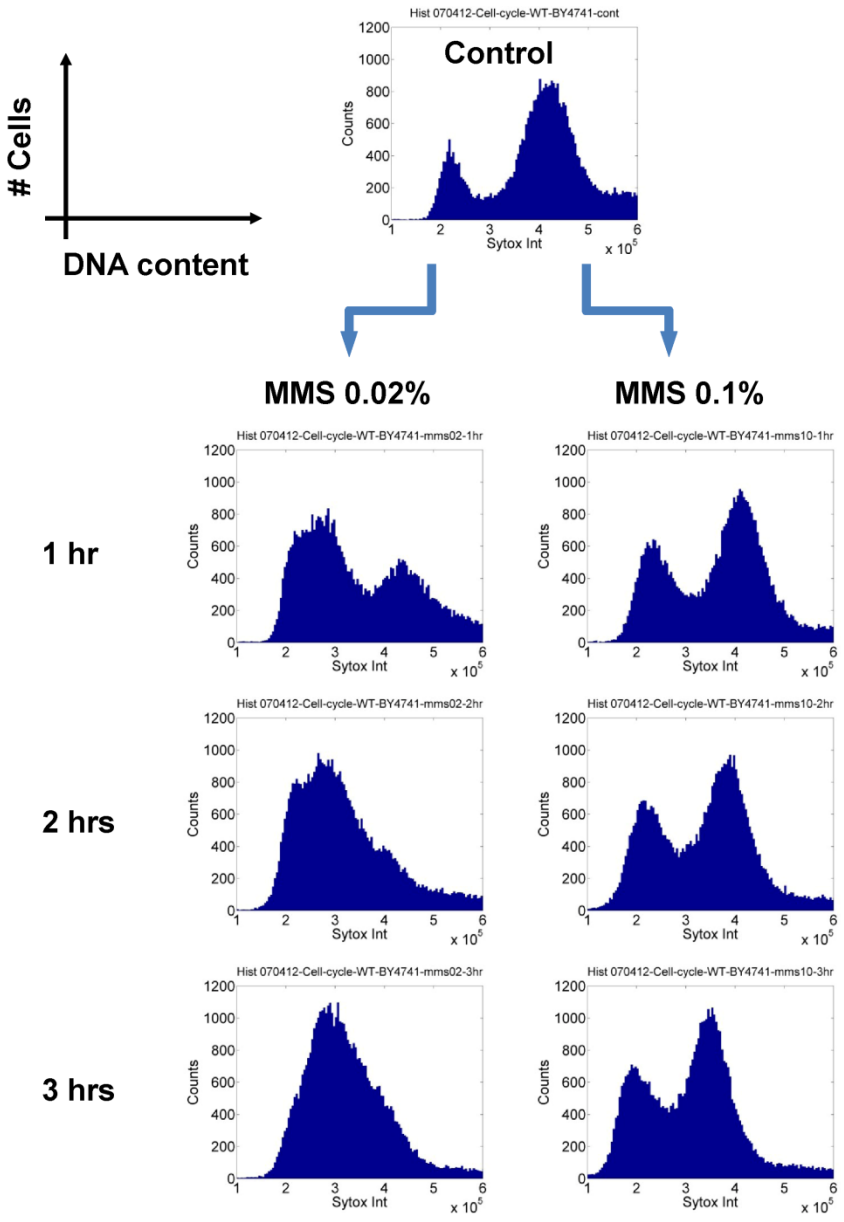

Supplementary Figure 19. Cell-cycle profiles at two different doses of MMS. An exponentially growing culture of WT BY4741 cells (Control), was treated with either 0.02% MMS or 0.1% MMS, for the times indicated on left. Cells were fixed in 70% ethanol and stained with 1 μM Sytox Green for flow cytometry following standard protocols (23). The cells treated with 0.02% MMS show a shift in the cell-cycle profiles as cells arrest in the S phase, repair damage and progress through the cell-cycle slowly. The cells treated with 0.1% MMS show almost no difference in cell-cycle distribution as the cells hit a complete stasis and halt growth.

References

1. (2006) *Green Fluorescent Protein: Properties, Applications, and Protocols*. 2 ed. John Wiley & Sons, Inc.
2. Tsien, R.Y. (1998) The green fluorescent protein. *Annu Rev Biochem*, **67**, 509-544.
3. Huh, W.K., Falvo, J.V., Gerke, L.C., Carroll, A.S., Howson, R.W., Weissman, J.S. and O'Shea, E.K. (2003) Global analysis of protein localization in budding yeast. *Nature*, **425**, 686-691.
4. Newman, J.R., Ghaemmaghami, S., Ihmels, J., Breslow, D.K., Noble, M., DeRisi, J.L. and Weissman, J.S. (2006) Single-cell proteomic analysis of S. cerevisiae reveals the architecture of biological noise. *Nature*, **441**, 840-846.
5. Brock, R., Hamelers, I.H. and Jovin, T.M. (1999) Comparison of fixation protocols for adherent cultured cells applied to a GFP fusion protein of the epidermal growth factor receptor. *Cytometry*, **35**, 353-362.
6. Rossanese, O.W., Soderholm, J., Bevis, B.J., Sears, I.B., O'Connor, J., Williamson, E.K. and Glick, B.S. (1999) Golgi structure correlates with transitional endoplasmic reticulum organization in Pichia pastoris and Saccharomyces cerevisiae. *J Cell Biol*, **145**, 69-81.
7. Baumstark-Khan, C., Palm, M., Wehner, J., Okabe, M., Ikawa, M. and Horneck, G. (1999) Green Fluorescent Protein (GFP) as a Marker for Cell Viability After UV-Irradiation. *Journal of Fluorescence*, **9**, 37-43.
8. Bence, N.F., Bennett, E.J. and Kopito, R.R. (2005) Application and analysis of the GFPu family of ubiquitin-proteasome system reporters. *Methods Enzymol*, **399**, 481-490.
9. Liu, Z., Meray, R.K., Grammatopoulos, T.N., Fredenburg, R.A., Cookson, M.R., Liu, Y., Logan, T. and Lansbury, P.T., Jr. (2009) Membrane-associated farnesylated UCH-L1 promotes alpha-synuclein neurotoxicity and is a therapeutic target for Parkinson's disease. *Proc Natl Acad Sci U S A*, **106**, 4635-4640.
10. Biggins, S., Severin, F.F., Bhalla, N., Sassoon, I., Hyman, A.A. and Murray, A.W. (1999) The conserved protein kinase Ipl1 regulates microtubule binding to kinetochores in budding yeast. *Genes Dev*, **13**, 532-544.
11. Ward, W.W. (2006) Biochemical and physical properties of green fluorescent protein. *Methods Biochem Anal*, **47**, 39-65.
12. Lee, M.W., Kim, B.J., Choi, H.K., Ryu, M.J., Kim, S.B., Kang, K.M., Cho, E.J., Youn, H.D., Huh, W.K. and Kim, S.T. (2007) Global protein expression profiling of budding yeast in response to DNA damage. *Yeast*, **24**, 145-154.
13. Giuliano, K.A., Chen, Y.T. and Taylor, D.L. (2004) High-content screening with siRNA optimizes a cell biological approach to drug discovery: defining the role of P53 activation in the cellular response to anticancer drugs. *J Biomol Screen*, **9**, 557-568.
14. Giuliano, K.A., Cheung, W.S., Curran, D.P., Day, B.W., Kassick, A.J., Lazo, J.S., Nelson, S.G., Shin, Y. and Taylor, D.L. (2005) Systems cell biology knowledge created from high content screening. *Assay Drug Dev Technol*, **3**, 501-514.
15. Giuliano, K.A., Johnston, P.A., Gough, A. and Taylor, D.L. (2006) Systems cell biology based on high-content screening. *Methods Enzymol*, **414**, 601-619.
16. Perlman, Z.E., Slack, M.D., Feng, Y., Mitchison, T.J., Wu, L.F. and Altschuler, S.J. (2004) Multidimensional drug profiling by automated microscopy. *Science*, **306**, 1194-1198.
17. Gorenstein, J., Zack, B., Marszalek, J.R., Bagchi, A., Subramaniam, S., Carroll, P. and Elbi, C. (2010) Reducing the multidimensionality of high-content screening into versatile powerful descriptors. *Biotechniques*, **49**, 663-665.
18. Malo, N., Hanley, J.A., Cerquozzi, S., Pelletier, J. and Nadon, R. (2006) Statistical practice in high-throughput screening data analysis. *Nat Biotechnol*, **24**, 167-175.

19. Wilson, C.J., Si, Y., Thompsons, C.M., Smellie, A., Ashwell, M.A., Liu, J.F., Ye, P., Yohannes, D. and Ng, S.C. (2006) Identification of a small molecule that induces mitotic arrest using a simplified high-content screening assay and data analysis method. *J Biomol Screen*, **11**, 21-28.
20. Pearson, E.S. and Hartley, H.O. (1972) *Biometrika Tables for Statisticians*. Camridge University Press, Cambridge.
21. Sheskin, D.J. (2000) *Handbook of Parametric and Nonparametric Statistical Procedures: Second Edition*. Chapman & Hall/CRC, Boca Raton.
22. Saville, D.J. (1990) Multiple Comparison Procedures: The Practical Solution. *The American Statistician*, **44**, 174-180.
23. Haase, S.B. and Reed, S.I. (2002) Improved flow cytometric analysis of the budding yeast cell cycle. *Cell Cycle*, **1**, 132-136.
24. Tkach, J.M., Yimit, A., Lee, A.Y., Riffle, M., Costanzo, M., Jaschob, D., Hendry, J.A., Ou, J., Moffat, J., Boone, C. *et al.* (2012) Dissecting DNA damage response pathways by analysing protein localization and abundance changes during DNA replication stress. *Nat Cell Biol*, **14**, 966-976.
25. Begley, U., Dyavaiah, M., Patil, A., Rooney, J.P., DiRenzo, D., Young, C.M., Conklin, D.S., Zitomer, R.S. and Begley, T.J. (2007) Trm9-catalyzed tRNA modifications link translation to the DNA damage response. *Mol Cell*, **28**, 860-870.
26. Fu, D. and Collins, K. (2006) Human telomerase and Cajal body ribonucleoproteins share a unique specificity of Sm protein association. *Genes Dev*, **20**, 531-536.
27. Agne, B., Infanger, S., Wang, F., Hofstetter, V., Rahim, G., Martin, M., Lee, D.W., Hwang, I., Schnell, D. and Kessler, F. (2009) A toc159 import receptor mutant, defective in hydrolysis of GTP, supports preprotein import into chloroplasts. *J Biol Chem*, **284**, 8670-8679.